Electronic Supplementary Material (ESI) for Nanoscale Advances.

Electronic Supplemental Information (ESI)

Title

Photo-responsive hole formation in the monolayer membrane wall of a supramolecular nanotube for quick recovery of encapsulated protein

Authors

N. Kameta,* Y. Kikkawa and Y. Norikane

An amphiphilic azobenzene derivative, **GlcAzo**, was synthesized in accordance with the scheme shown in Figure S1. 2,3,4,6-Tetra-*O*-acetyl-β-$_D$-glucopyranosyl amine was prepared by using a method reported previously (*Langmuir*, 2004, **20**, 5969). Azobenzene-4-carbonyl chloride was purchased from Tokyo Chemical Industry. Condensation reaction between 2,3,4,6-tetra-*O*-acetyl-β-$_D$-glucopyranosyl amine (0.94 g, 2.7 mmol) and azobenzene-4-carbonyl chloride (0.66 g, 2.7 mmol) in dimethyl formamide (50 mL) in the presence of triethylamine (0.27 g, 2.7 mmol) afforded precursor **1** as a precipitate (1.22 g, 2.2 mmol, 81% yield). Addition of NaOMe (0.48 g, 8.8 mmol) to a methanol solution of **1** (1.22 g, 2.2 mmol) removed the acetyl groups from **1**. **GlcAzo** precipitated from the methanol solution was recovered by filtration and washed several times with methanol (0.62 g, 1.6 mmol, 73% yield).

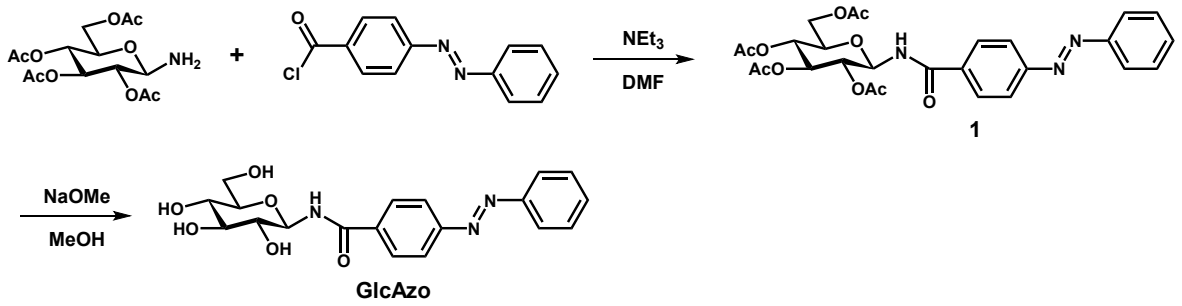

Figure S1. Synthetic scheme of **GlcAzo**.

1: ^{1}H NMR (400 MHz, DMSO-d_6, 25 °C): δ = 8.14 (d, J = 8.7 Hz, 2H; Azo), 8.02 (d, J = 8.7 Hz, 2H; Azo), 7.95 (dd, J = 7.4 and 3.6 Hz, 2H; Azo), 7.64 (overlap, 3H; Azo), 6.25 (d, J = 8.2 Hz, 1H; Glc-1), 5.57 (t, J = 9.6 Hz, 1H; Glc-3), 5.17 (t, J = 8.3 Hz, 1H; Glc-2), 5.06 (t, J = 9.6 Hz, 1H; Glc-4), 4.34 (m, 1H; Glc-5), 4.22 (dd, J = 12.5 and 4.7 Hz, 1H; Glc-6), 4.05 (dd, J = 12.5 and 1.9 Hz, 1H; Glc-6), 2.02 (s, 3H; OAc), 2.01 (s, 1H; OAc), 1.99 (s, 1H; OAc), 1.98 (s, 1H; OAc), no peak attributable to NH was observed.

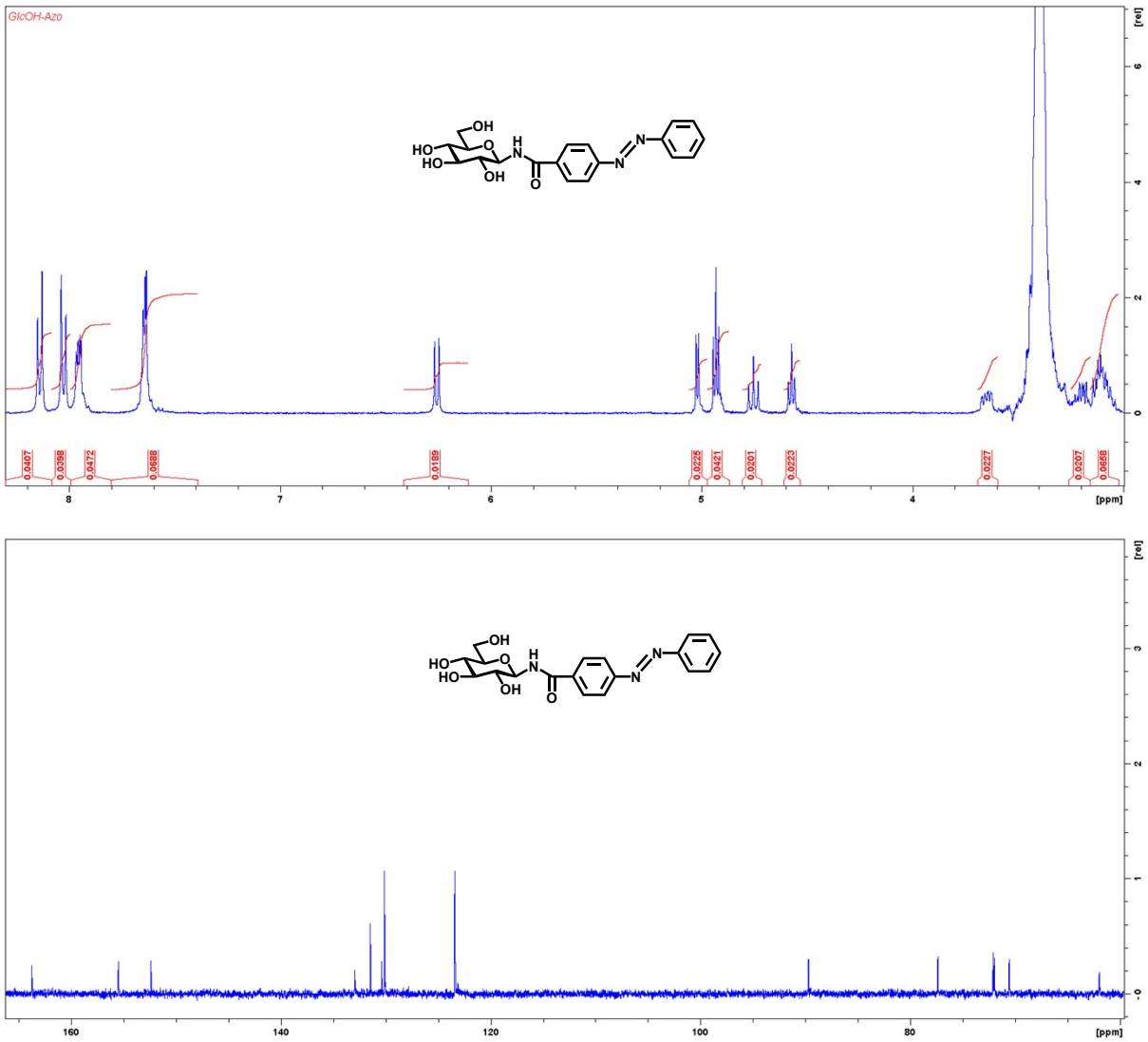

Figure S2. ^{1}H and ^{13}C nuclear magnetic resonance spectra of **GlcAzo** in DMSO-d_6 at 25 °C.

GlcAzo: ^{1}H NMR (400 MHz, DMSO-d_6, 25 °C): δ = 8.14 (d, J = 8.7 Hz, 2H; Azo), 8.03 (d, J = 8.7 Hz, 2H; Azo), 7.96 (dd, J = 7.4 and 3.6 Hz, 2H; Azo), 7.65 (overlap, 3H; Azo), 6.25 (d, J = 8.2 Hz, 1H; NH), 5.01 (d, J = 4.7 Hz, 1H; Glc-4-OH), 4.94 (d, J = 5.2 Hz, 1H; Glc-3-OH), 4.92 (d, J = 5.1 Hz, 1H; Glc-2-OH), 4.75 (t, J = 9.0 Hz, 1H; Glc-1), 4.57 (t, J = 5.9 Hz, 1H; Glc-6-OH), 3.64 (dd, J = 10.2 and 5.9 Hz, 1H; Glc-6), 3.4 (overlapped with water, 1H; Glc-6), 3.20 (m, 1H; Glc-4), 3.04–3.23 (overlap, 3H; Glc-2, Glc-3, and Glc-5). ^{13}C NMR (400 MHz, DMSO-d_6, 25 °C): δ = 163.8 (1C; C=O), 155.5 (1C; Azo), 152.4 (1C; Azo), 133.0 (1C; Azo), 131.5 (2c; Azo), 130.4 (1C; Azo), 130.1 (2C; Azo), 123.4 (4C; Azo), 89.4 (1C; Glc-1), 77.4 (1C; Glc-5), 73.3 (2C; Glc-3 and Glc-2); 71.1 (1C; Glc-4), 62.2 (1C; Glc-6). ESI-MS (anionic mode) m/z: 386.1 $[M - H]^-$. Anal. calcd for $C_{19}H_{21}N_3O_6$: C 58.91, H 5.46, N 10.85; found: C 58.83, H 5.45, N 10.81.

An amphiphilic azobenzene derivative, **GlcGlyAzo**, was synthesized in accordance with the scheme shown in Figure S3. Z-Gly-OSu was purchased from Bachem. Condensation reaction between 2,3,4,6-tetra-*O*-acetyl-β-$_D$-glucopyranosyl amine (1.88 g, 5.4 mmol) and Z-Gly-OSu (1.64 g, 5.4 mmol) was performed in dry methanol (100 mL). After evaporation of the solvent, the residue was washed with 5% citric acid and 10% $NaHCO_3$. The obtained solid was treated with Pd/C and H_2 gas in methanol to deprotect the benzyloxycarbonyl (Z) group. After removal of Pd/C by filtration, azobenzene-4-carbonyl chloride (1.32 g, 5.4 mmol) was added to the resultant methanol solution. After evaporation of the solvent, the residue was subjected to silica gel column chromatography (eluent solution, hexane:ethyl acetate = 50%:50%). The yield of the isolated compound, **2**, was 31% (1.04 g, 1.7 mmol). Addition of NaOMe (0.37 g, 6.8 mmol) into a methanol solution of **2** (1.04 g, 1.7 mmol) removed the acetyl groups from **2**. **GlcGlyAzo** precipitated from the methanol solution was recovered by filtration and washed several times with methanol (0.49 g, 1.1 mmol, 66% yield).

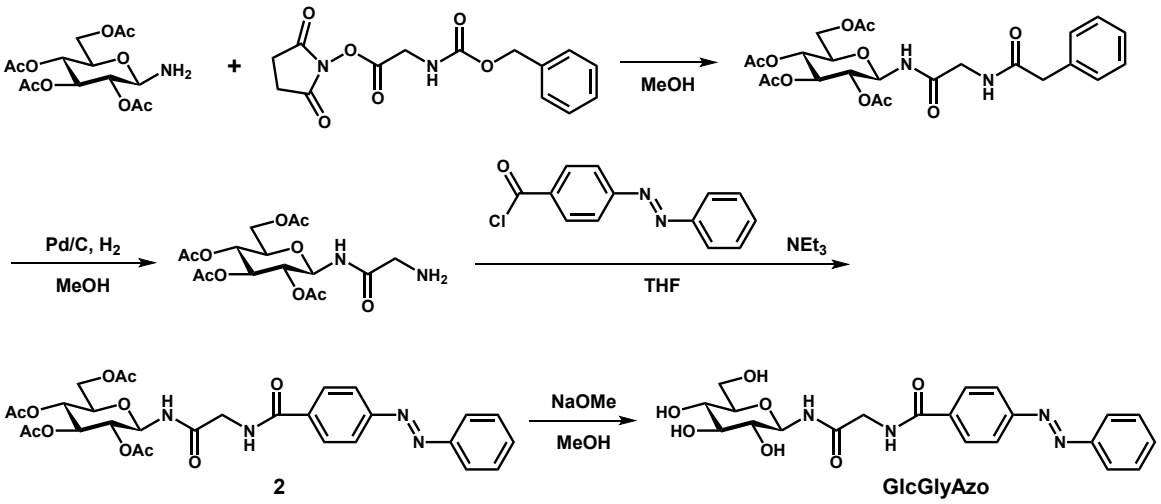

Figure S3. Synthetic scheme of **GlcGlyAzo**.

2: ^{1}H NMR (400 MHz, DMSO-d_6, 25 °C): δ = 8.93 (t, *J* = 5.8 Hz, 1H; NH), 8.75 (t, *J* = 9.4 Hz, 1H; NH), 8.08 (d, *J* = 8.5 Hz, 2H; Azo), 7.97 (d, *J* = 8.5 Hz, 2H; Azo), 7.94 (dd, *J* = 8.0 and 2.1 Hz, 2H; Azo), 7.62 (overlap, 3H; Azo), 5.44 (t, *J* = 9.4 Hz, 1H; Glc-1), 5.36 (t, *J* = 9.5 Hz, 1H; Glc-3), 4.91 (t, *J* = 9.4 Hz, 1H; Glc-2), 4.88 (t, *J* = 9.3 Hz, 1H; Glc-4), 4.15 (dd, *J* = 12.2 and 4.5 Hz, 1H; Glc-6), 4.12 (m, 1H; Glc-5), 3.99 (d, *J* = 10.9 Hz, 1H; Glc-6), 3.89 (dd, *J* = 6.4 and 3.3 Hz, 2H; Gly), 2.01 (s, 3H; OAc), 1.99 (s, 1H; OAc), 1.98 (s, 1H; OAc), 1.93 (s, 1H; OAc).

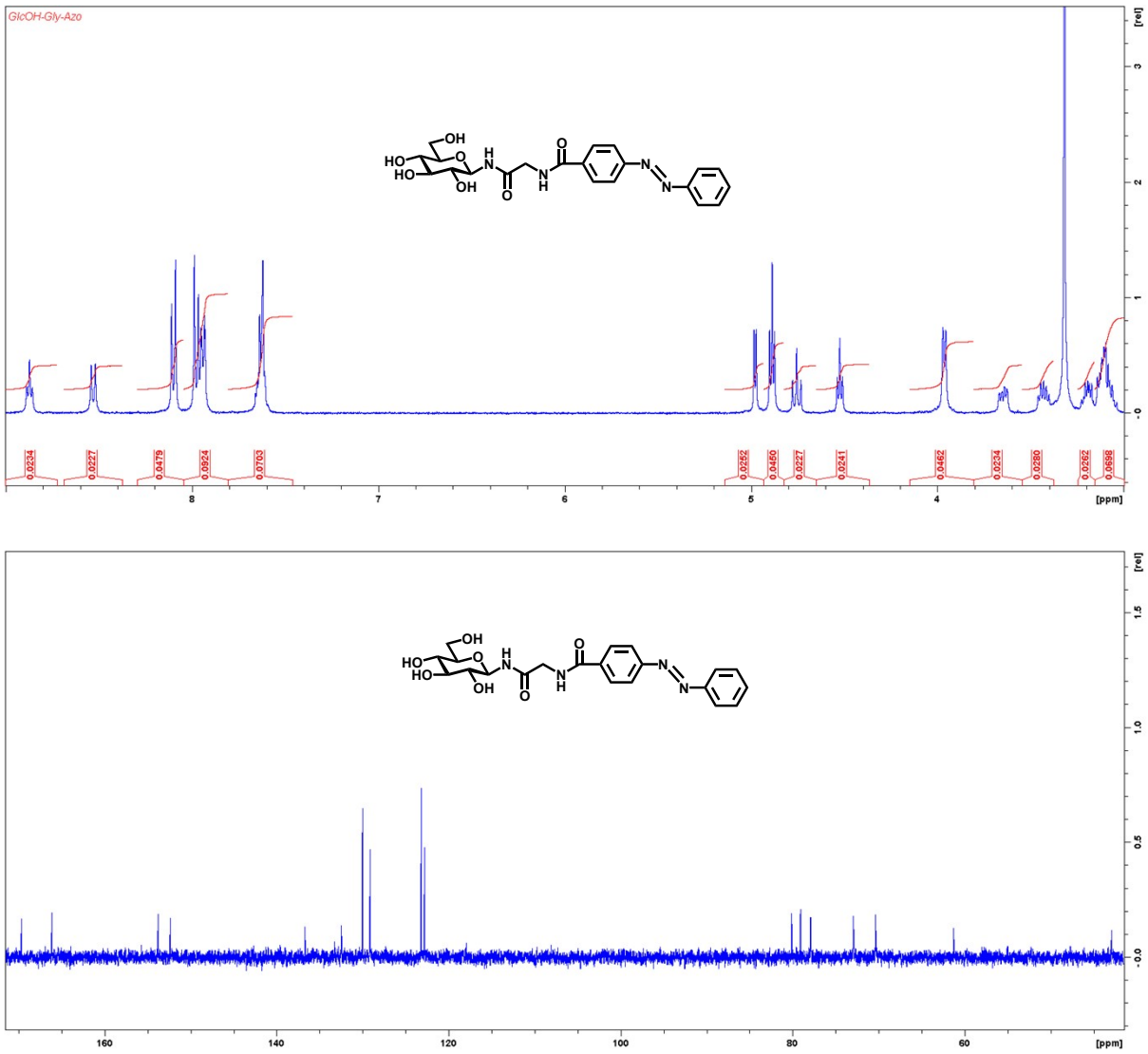

Figure S4. ^{1}H and ^{13}C nuclear magnetic resonance spectra of **GlcGlyAzo** in DMSO-d_6 at 25 °C.

GlcGlyAzo: ^{1}H NMR (400 MHz, DMSO-d_6, 25 °C): δ = 8.87 (t, J = 5.8 Hz, 1H; NH), 8.53 (t, J = 9.0 Hz, 1H; NH), 8.09 (d, J = 8.6 Hz, 2H; Azo), 7.97 (d, J = 8.6 Hz, 2H; Azo), 7.94 (dd, J = 8.0 and 2.2 Hz, 2H; Azo), 7.62 (overlap, 3H; Azo), 4.98 (d, J = 4.7 Hz, 1H; Glc-4-OH), 4.89 (d, J = 5.4 Hz, 1H; Glc-3-OH), 4.88 (d, J = 5.3 Hz, 1H; Glc-2-OH), 4.75 (t, J = 9.0 Hz, 1H; Glc-1), 4.52 (t, J = 5.7 Hz, 1H; Glc-6-OH), 3.96 (d, J = 5.9 Hz, 2H; Gly), 3.64 (dd, J = 10.2 and 5.7 Hz, 1H; Glc-6), 3.43 (dd, J = 11.3 and 5.4 Hz, 1H; Glc-6), 3.20 (m, 1H; Glc-4), 3.14–3.03 (overlap, 3H; Glc-2, Glc-3, and Glc-5). ^{13}C NMR (400 MHz, DMSO-d_6, 25 °C): δ = 169.7 (1C; C=O), 166.2 (1C; C=O), 153.8 (1C; Azo), 152.4 (1C; Azo), 136.8 (1C; Azo), 132.5 (1c; Azo), 130.0 (2C; Azo), 129.2 (2C; Azo), 123.2 (2C; Azo), 122.8 (2C; Azo), 80.2 (1C; Glc-1), 79.1 (1C; Glc-5), 77.9 (1C; Glc-3); 73.0 (1C; Glc-2), 70.4 (1C; Glc-4), 61.3 (1C;

Glc-6), 42.9 (1C; Gly). ESI-MS (anionic mode) *m*/*z*: 443.1 $[M - H]^-$. Anal. calcd for $C_{21}H_{24}N_4O_7$: C 56.75, H 5.44, N 12.61; found: C 56.59, H 5.51, N 12.53.

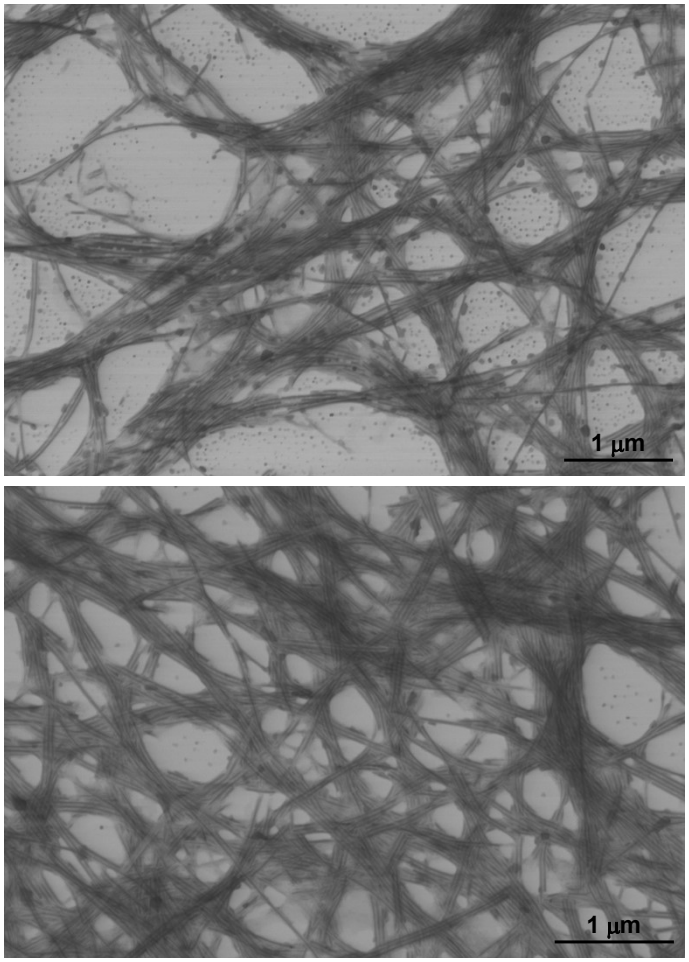

Figure S5. Representative scanning transmission electron micrographs of $GlcC_{18}$-GlcAzo-tubes (upper) and $GlcC_{18}$-GlcGlyAzo-tubes (lower). The images revealed the formation of nanotubes but not of GlcAzo-sheet or GlcGlyAzo-tape.

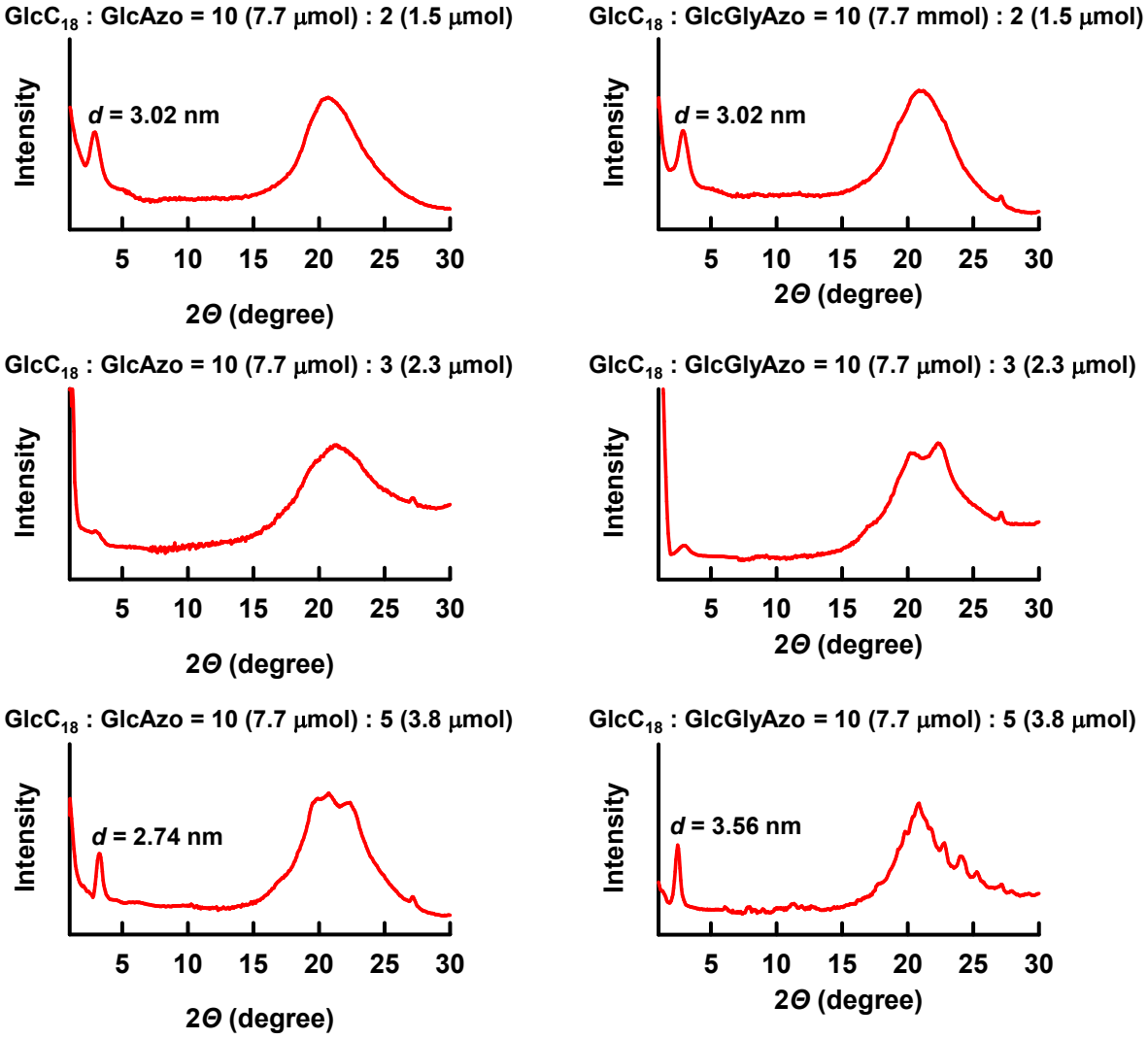

Figure S6. Powder X-ray diffraction patterns of nanostructures formed by binary self-assembly of $GlcC_{18}$ and GlcAzo or GlcGlyAzo at different molar ratios. The *d* values 3.02, 2.74, and 3.56 nm correspond to the stacking periodicity of $GlcC_{18}$ in $GlcC_{18}$-tube, GlcAzo in GlcAzo-sheet and GlcGlyAzo in GlcGlyAzo-tape, respectively. No peaks in the wide-angle region of the middle two patterns indicate that all of the azobenzene derivatives were incorporated into $GlcC_{18}$-tube without the formation of GlcAzo-sheet or GlcGlyAzo-tape or of $GlcC_{18}$-tube containing no azobenzene derivative. $GlcC_{18}$-GlcAzo-tube and $GlcC_{18}$-GlcGlyAzo-tube consist of a single monolayer membrane and therefore have no *d* spacing.

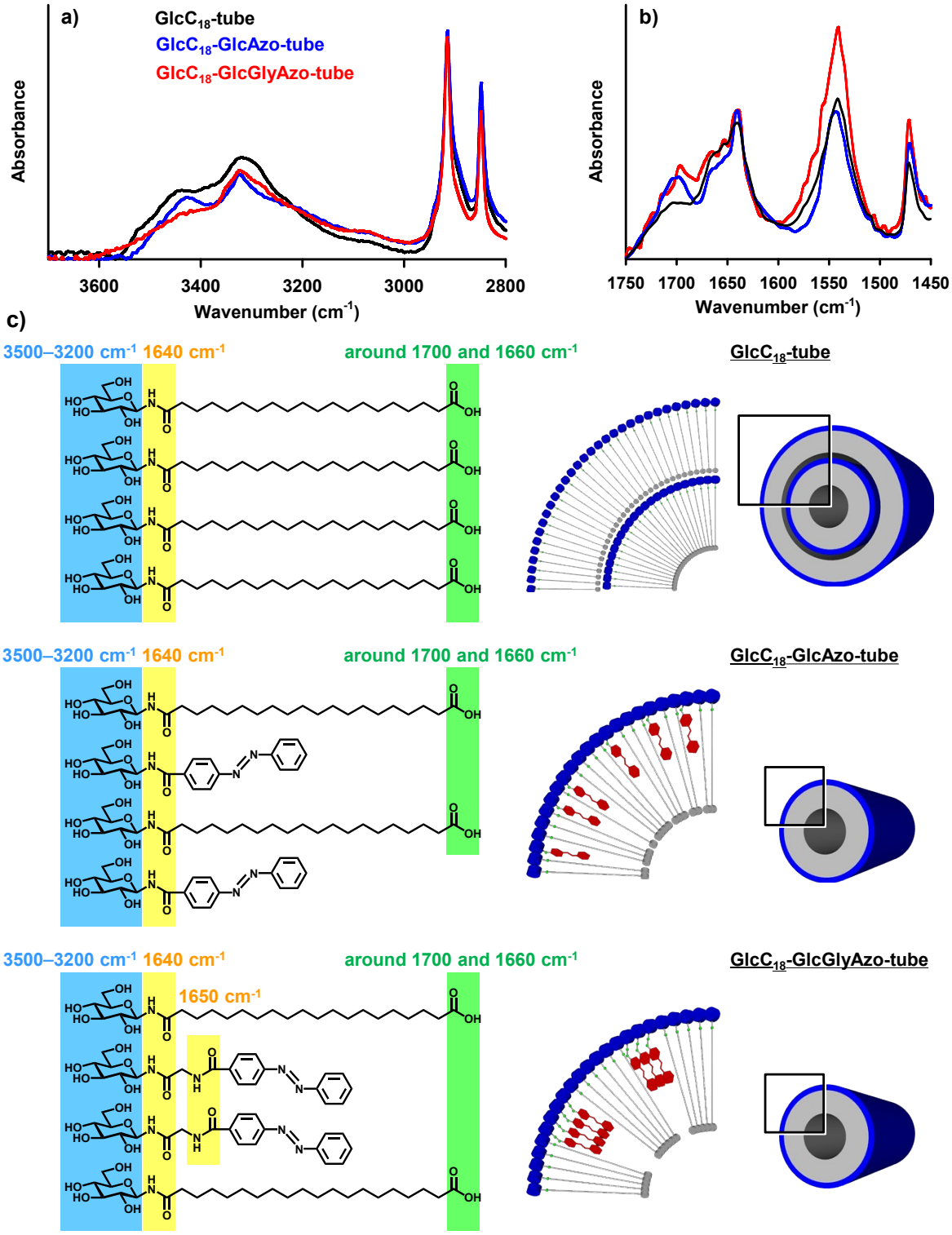

Figure S7. (a) The O-H stretching infrared band of the glucose headgroup and (b) the C=O stretching infrared band of the amide and carboxyl groups in the indicated nanotubes. (c) Schematic representation of the molecular packing of the indicated nanotubes. Blue, yellow, and green bands show the different intermolecular hydrogen bond networks.

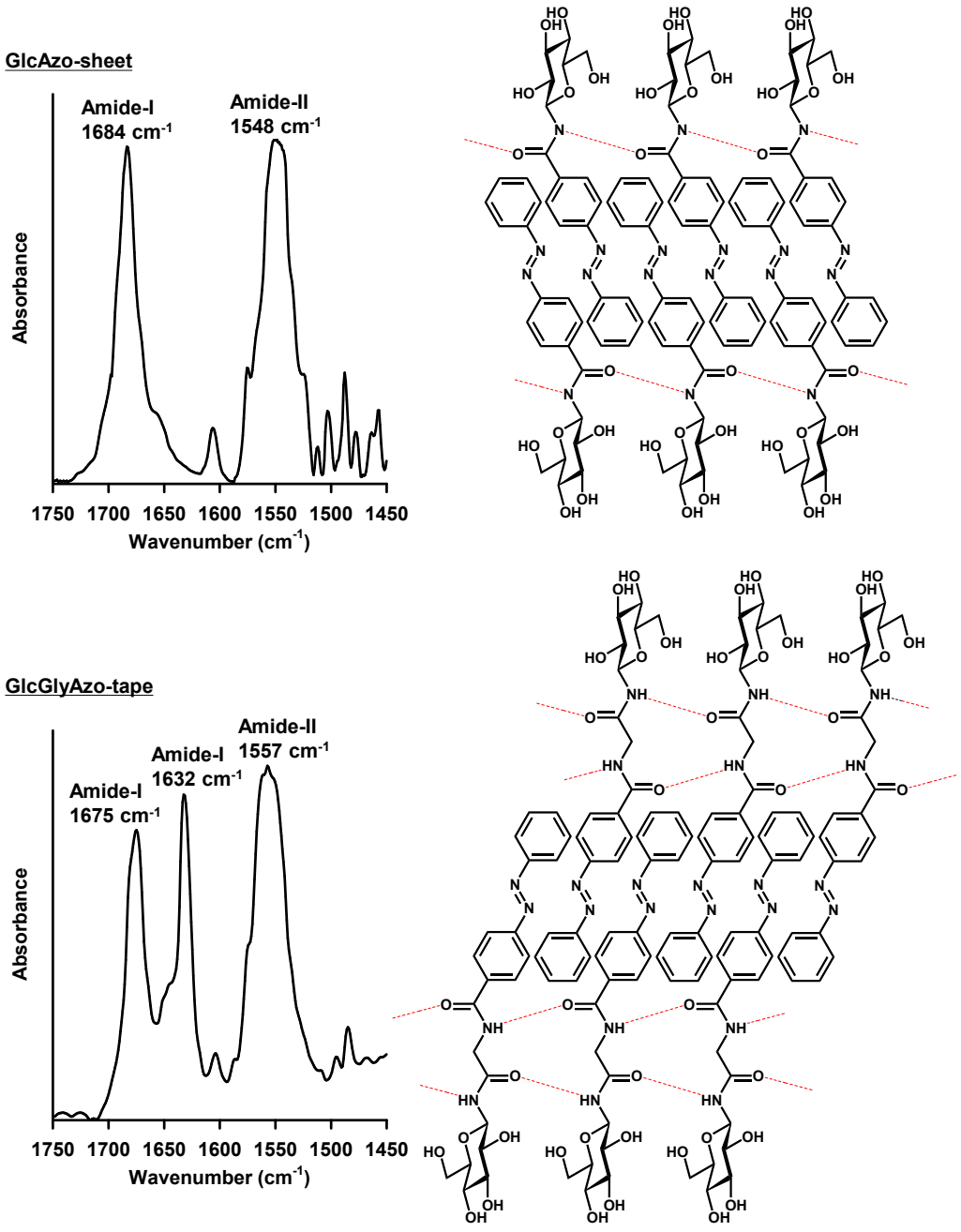

Figure S8. Left: Amide-I and -II infrared spectra of GlcAzo-sheet and GlcGlyAzo-tape. Right: Schematic representation of the intermolecular hydrogen bond network in GlcAzo-sheet and GlcGlyAzo-tape.

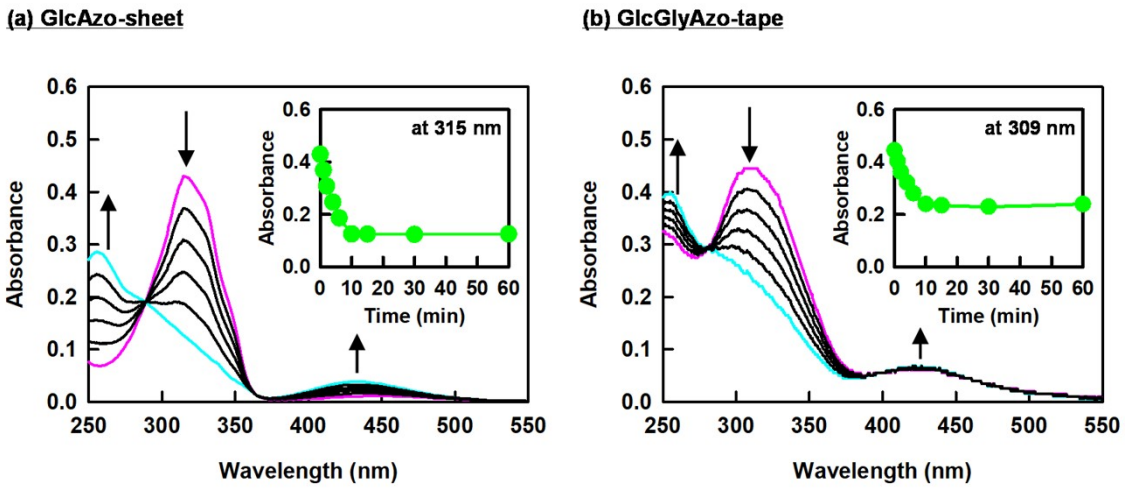

Figure S9. Changes in absorption spectra upon ultraviolet irradiation of (a) GlcAzo-sheet or (b) GlcGlyAzo-tape dispersed in water. The pink and blue spectra were recorded before ultraviolet irradiation and after ultraviolet irradiation for 10 min, respectively. Insets show the relationship between the absorbance at the maximum wavelength and ultraviolet irradiation time. [GlcAzo] = [GlcGlyAzo] = 2.3×10^{-4} M.

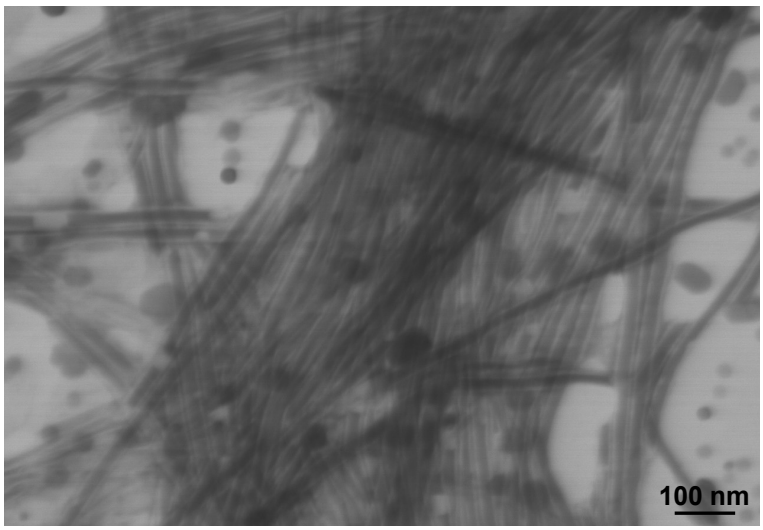

Figure S10. Scanning transmission electron micrographs of $GlcC_{18}$-GlcGlyAzo-tubes after ultraviolet irradiation for 5 min. The image confirmed that the hole formation upon ultraviolet irradiation does not influence the basic tubular morphology such as the inner diameter size and the wall thickness.

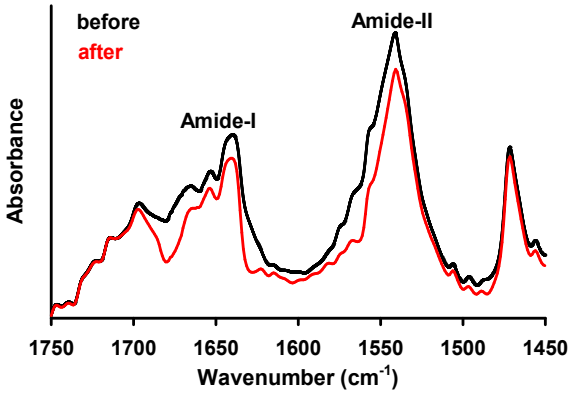

Figure S11. The C=O stretching infrared band of the amide groups in $GlcC_{18}$-GlcGlyAzo-tubes before and after ultraviolet irradiation for 5 min. The spectra revealed that the hole formation upon ultraviolet irradiation does not influence the intermolecular hydrogen bonding among $GlcC_{18}$ within the monolayer membrane.

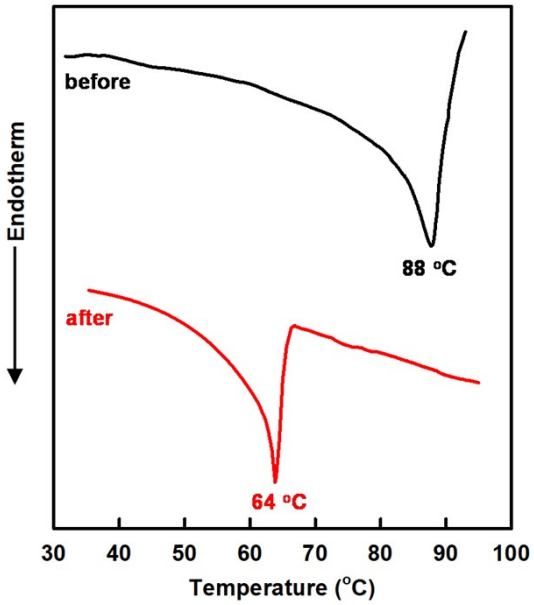

Figure S12. Differential scanning calorimetry profiles of hydrated $GlcC_{18}$-GlcGlyAzo-tubes before and after ultraviolet irradiation for 5 min. Decomposition temperatures estimated from the endothermic peaks revealed that the thermal stability of $GlcC_{18}$-GlcGlyAzo-tube remarkably decreases after the hole formation upon ultraviolet irradiation.

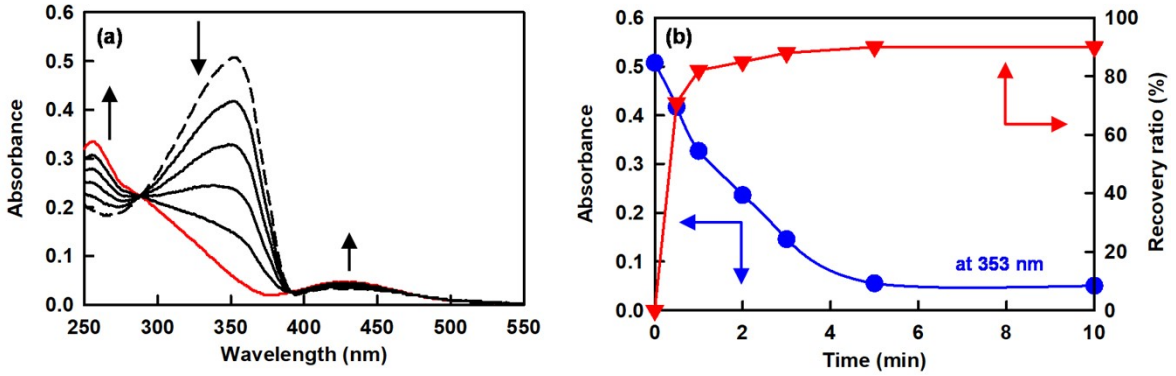

Figure S13. (a) Changes in absorption spectra upon ultraviolet irradiation of $GlcC_{18}$-GlcGlyAzo-tube dispersed in water. The black dot and red spectra were recorded before ultraviolet irradiation and after ultraviolet irradiation for 5 min, respectively. (b) Time dependence of the variation of the absorbance at the maximum wavelength (extracted from (a)) and the recovery ratios of the GlcGlyAzo component of $GlcC_{18}$-GlcGlyAzo-tube.